Supplementary document

Thermal activation significantly improves the organic pollutant removal rate of low-grade manganese ore in peroxymonosulfate system

Yi Chen [a], Ping Yin [b], Shuai Dong [a], Shiyue Wei [a], Jinchuan Gu [a]*, Wanglai Cen [c]

[a] School of Food and Bioengineering, Civil Engineering and Architecture and Environment, Xihua University, Chengdu, 610039, PR China

[b] Sichuan Rongxinkai Engineering Design Co.Ltd., Chengdu, 610041, PR China

[c] National Engineering Research Center for Flue Gas Desulfurization, Sichuan University, Chengdu 610065, China

*Corresponding author: *Jinchuan Gu*; E-mail address: gu6471@163.com

Text 1. Effects of operational parameters

1. Effect of initial concentration

As shown in **Figure S9**(a), when the AO7 initial concentrations (C_0) were 20 mg/L and 40 mg/L, the AO7 removal efficiencies in the CNMO/PMS system were similar, reaching 99.1%-99.2%, with the fastest reaction rate (k_{obs}), 0.1056 min^{-1}, obtained when C_0 was 20 mg/L (**Figure S5**(a)). However, with the increase of C_0, the AO7 removal efficiency and k_{obs} in the CNMO/PMS system decreased significantly. This could be mainly attributed to the fact that, as the initial concentration of AO7 increased, the ROS provided by a certain amount of PMS became insufficient, thus reducing degradation efficiency[1].

2. Effects of catalyst dosage

More active sites can decompose more PMS into ROS in a given time, which is conducive to promoting the degradation of pollutants. In this study, when the catalyst dosage (M_{CNMO}) increased from 0.5 g/L to 1.5 g/L, the k_{obs} and removal efficiency increased obviously (**Figure S5**(b) and **Figure S9**(b)), reaching 2.09 times and 1.31 times of 0.5 g/L, respectively. The rate of ROS generation accelerated with the increased CNMO, possibly suggesting the reason for the remarkable degradation effect on AO7[2]. However, AO7 removal efficiency did not change significantly when M_{CNMO} was greater than 1.5 g/L, possibly limited by the PMS dosage (M_{PMS}) of the CNMO/PMS system.

3. Effect of PMS dosage

The effect of M_{PMS} (0.08-0.46 mM) was subsequently investigated to ascertain the most suitable amount of oxidant for AO7 degradation in the CNMO/PMS system. The AO7 removal efficiency and k_{obs} increased with the increase in M_{PMS} (**Figure S9**(c)). When the M_{PMS} was 0.46 mM, AO7 removal efficiency reached 98.11%, with k_{obs} at 0.1134 min^{-1}, indicating that PMS dosage was the limiting factor in the removal of AO7. Previous studies have reported that more PMS can enhance mass transfer between CNMO and PMS, resulting in a greater concentration of ROS for the removal of AO7[3, 4].

4. Effect of initial pH

Generally, the influence of different initial pH levels on the catalytic system cannot be ignored. As shown in **Figure S7**(d), the CNMO/PMS system maintained a high AO7 removal rate (> 97.50%) under both strong acid (pH = 2) and strong base (pH = 9) conditions. Even at pH = 11, the removal rate of the CNMO/PMS system was still able to reach 88.67%. The results indicate that CNMO has excellent PMS activation performance within a wide initial pH range (pH = 2-11), thereby deeming it a good prospect for practical application.

5. Effect of reaction temperature

The effect of reaction temperature on AO7 degradation in the CNMO/PMS system is shown in **Figure S7**(e) and **Figure S5**(e). As the temperature increased from 15 °C to 45 °C, the removal rate and k_{obs} increased, with the k_{obs} significantly enhanced from 0.0665 min^{-1} to 0.1431 min^{-1}, thus demonstrating that reaction temperature exerts a notable influence on AO7 degradation in the CNMO/PMS system. In addition, as shown in the plot of ln(k_{obs}) versus 1000/T (**Figure S7**(f)), when the E_a of AO7 in the system was calculated using the Arrhenius equation (Eq. (2)) it was found to be 20.62 kJ mol^{-1}, which is lower than previously reported values[1, 2] and demonstrated the ease of activation of PMS by CNMO.

Text 2. Measurement of oxidative intermediate species

In order to further understand the AO7 degradation pathway, the intermediates in the AO7 degradation process were analyzed by GCMS-QP2020NX, with eight intermediates detected (**Table S4**). First, the $^1O_2$ generated in the CNMO/PMS system attacked the -N=N- of AO7 and broke the bond, thereby forming 1-amino-2-naphthol and 4-aminobenzenesulfonic acid. Thereafter, the 1-amino-2-naphthol was oxidized to form P1/P2/P3 (Pathway I), while 1-amino-2-naphthol was oxidized to P4-P6 and, finally, to P7 and P8 (Pathway II). Finally, these intermediates of AO7 degradation could further react with ROS and convert into CO_2 and H_2O (**Figure S10**).
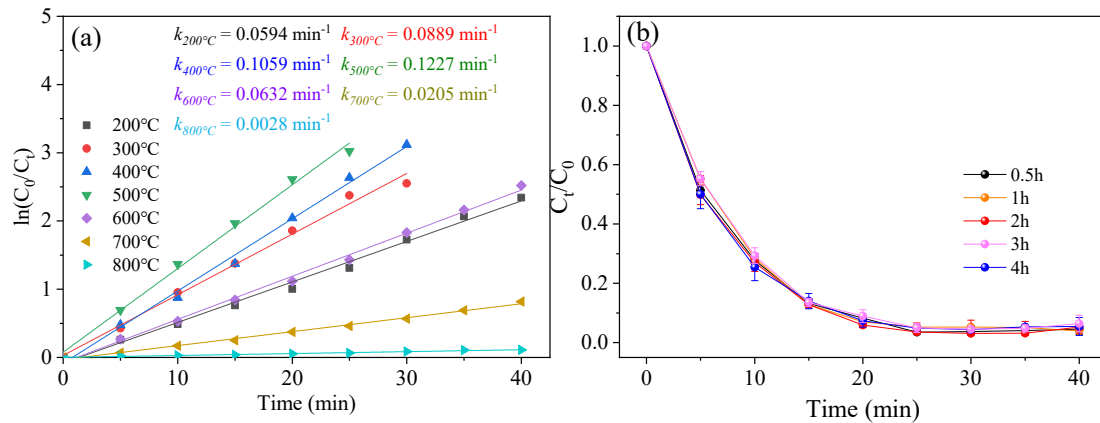
Figure S1. $\ln(C_0/C_t)$ versus time plot for degradation of AO7 by NMO thermal activation after different temperature (a) and the effect of catalyst calcination time on AO7 removal efficiency (b) (Conditions: C_0 = 20 mg/L, M_{GBO} = 0.9 g/L, M_{PMS} = 0.15 mM, pH = 6.6, T = 25 °C).
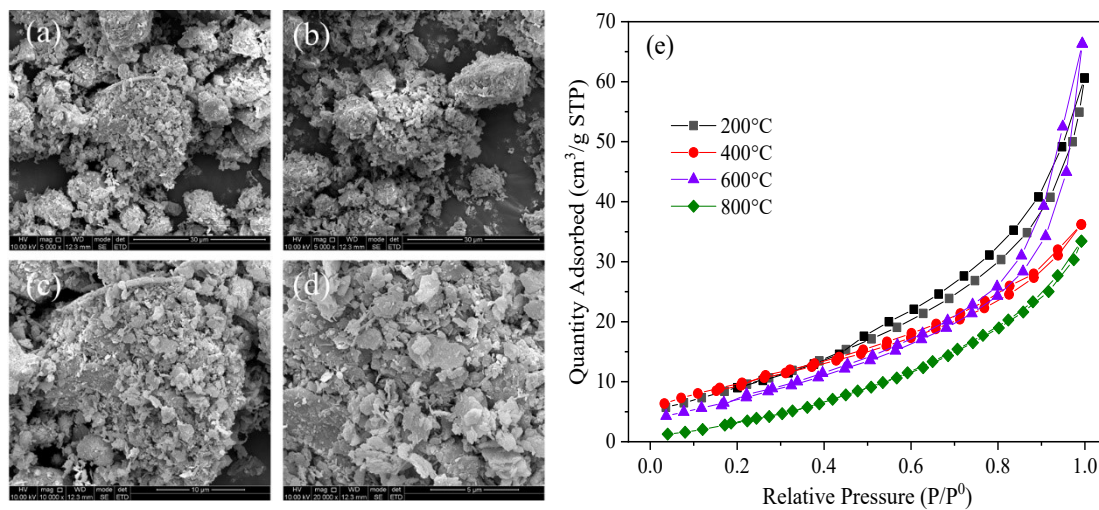

Figure S2. (a-d) SEM micrograph of NMO, (e) the N_2 adsorption-desorption isotherm of NMO calcined after different temperature.
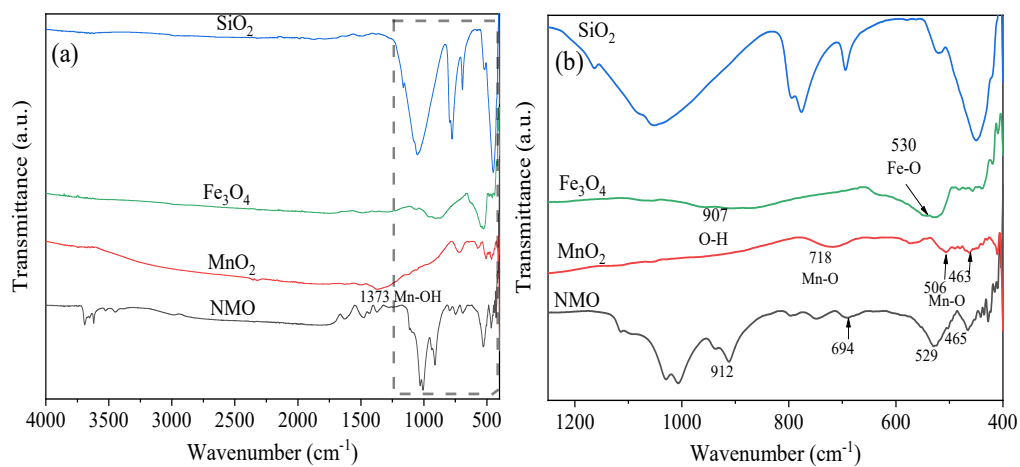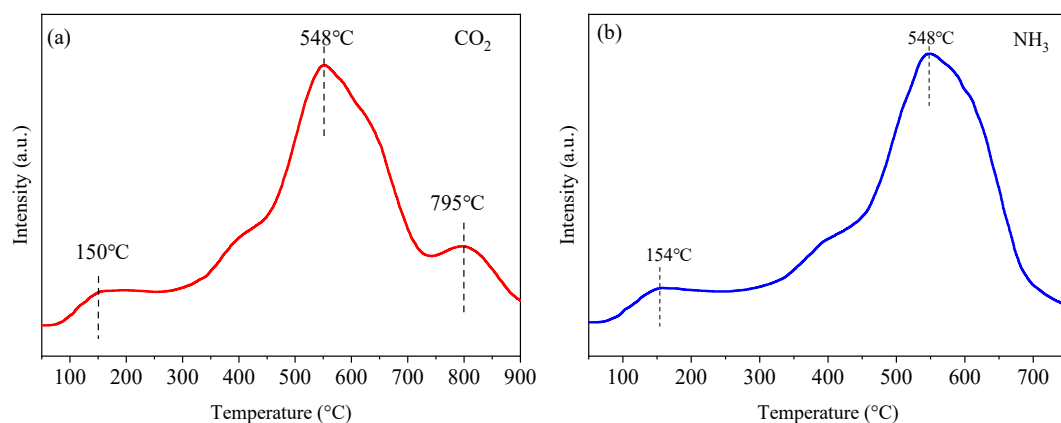

Figure S3. FTIR spectrum of NMO, pure MnO_2, Fe_3O_4 and SiO_2.

Figure S4. (a) CO_2-TPD and (b) NH_3-TPD of NMO.
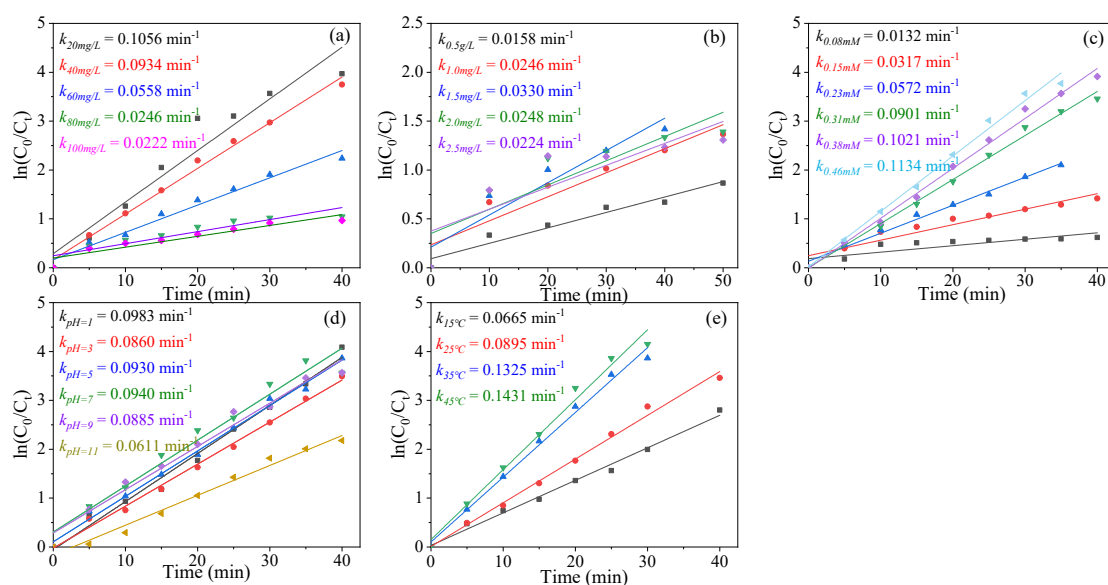
Figure S5. $\ln(C_0/C_t)$ versus time plot for degradation of AO7 by CNMO at different initial concentration (20-100 mg/L, M_{CNMO} = 0.9 g/L, M_{PMS} = 0.15 mM) (a), Catalyst dosage (0.5-2.5 mg/L, M_{PMS} = 0.15 mM) (b), PMS dosage (0.08-0.46 mM) (c), initial pH (pH = 1-11) (d) and reaction temperature (15-45 °C) (e). (Conditions: C_0 = 100 mg/L, M_{CGO} = 1.5 g/L, M_{PMS} = 0.31 mM, pH = 6.6, T = 25°C)
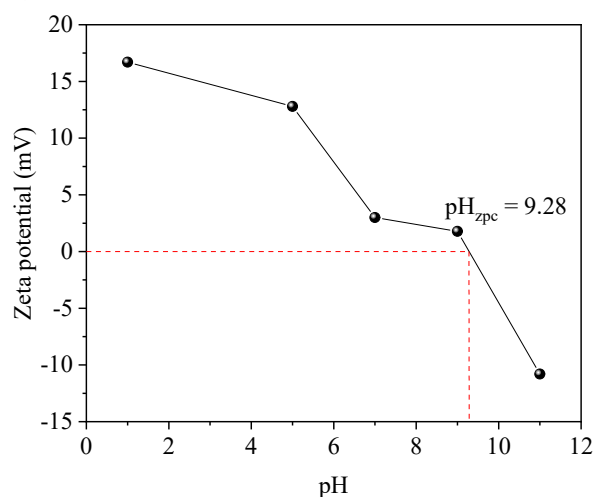
Figure S6. pH$_{zpc}$ of the CNMO by Zeta potential method.
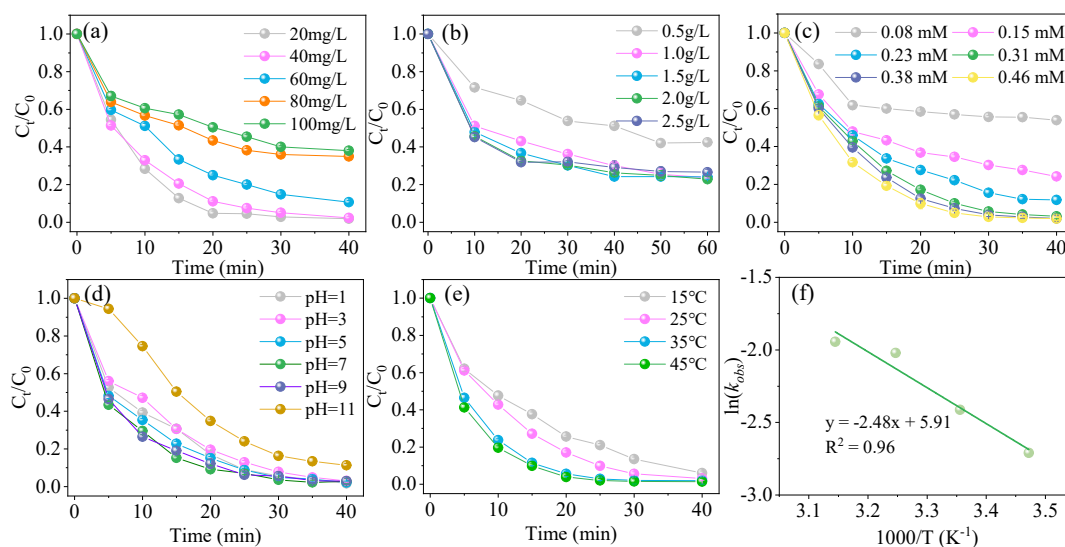
Figure S7. Effect of different experimental parameters on AO7 removal efficiency: (a) Initial concentration (20-100 mg/L, M$_{CNMO}$ = 0.9 g/L, M$_{PMS}$ = 0.15 mM) (b); catalyst dosages (0.5-2.5 mg/L, M$_{PMS}$ = 0.15 mM); (c) PMS dosage (0.08-0.46 mM); (d) initial pH (pH = 1-11); (e) reaction temperatures (15-45 °C); and (f) the plot of ln(k_{obs}) versus 1000/T in the CNMO/PMS oxidation. (Conditions: C$_0$ = 100 mg/L, M$_{CNMO}$ = 1.5 g/L, M$_{PMS}$ = 0.31 mM, pH = 6.6, T = 25 °C)
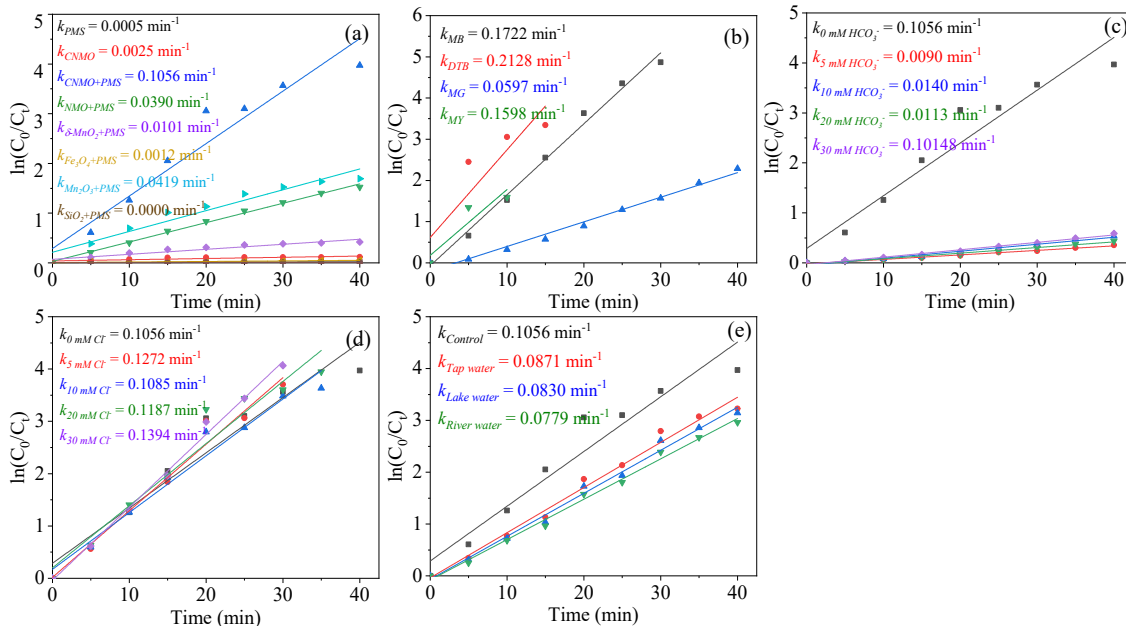
Figure S8. ln(C$_0$/C$_t$) versus time plot for degradation of AO7 in various systems (a), degradation of different pollutants in the CNMO/PMS system (b), degradation of AO7 in system contained HCO$_3^-$ (c) and Cl$^-$ (d), AO7 removal in actual water (e). (Conditions: C$_0$ = 20 mg/L, M$_{GBO}$ = 0.9 g/L, M$_{PMS}$ = 0.15 mM, pH = 6.6, T = 25 °C).
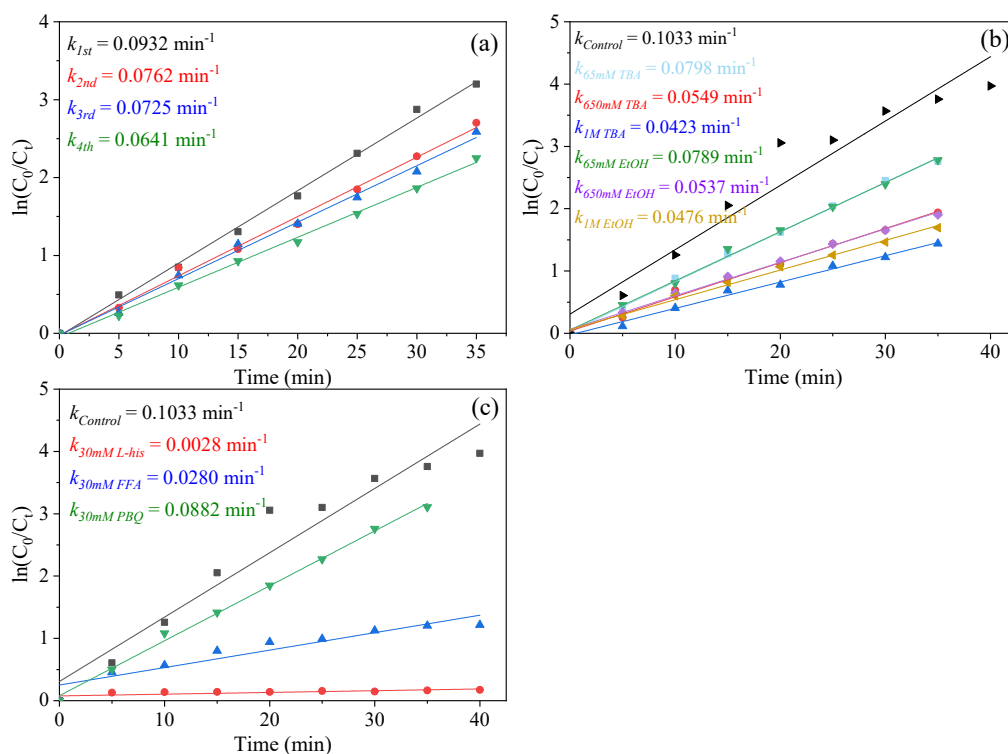
Figure S9. $\ln(C_0/C_t)$ versus time plot for degradation of AO7 in each recycling process (a), in the CNMO/PMS system under different quenching conditions (b-c). (Conditions: $C_0 = 100$ mg/L, $M_{CNMO} = 1.5$ g/L, $M_{PMS} = 0.31$ mM, pH = 6.6, T = 25 °C)
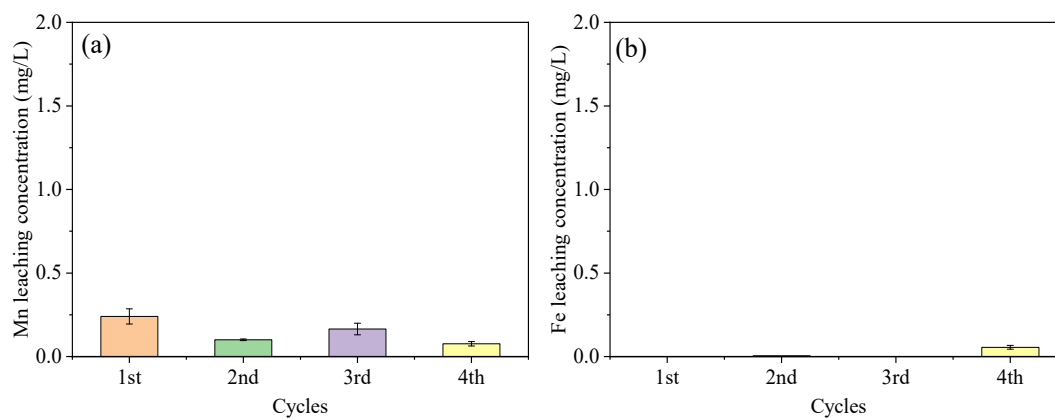

Figure S10. Mn (a) and Fe (b) leaching concentration in each recycling process. (Conditions: $C_0 = 100$ mg/L, $M_{CGO} = 1.5$ g/L, $M_{PMS} = 0.31$ mM, pH = 6.6 T = 25°C)
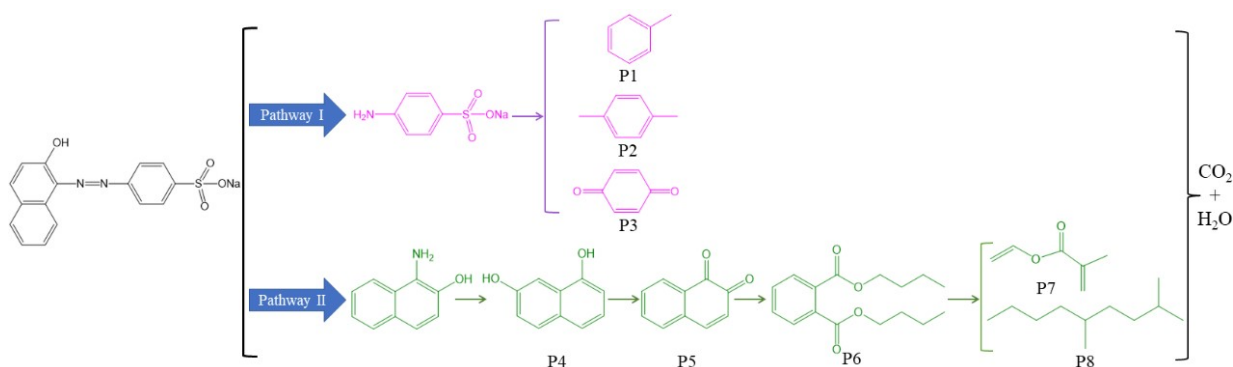

Figure S11. Degradation pathways of AO7 in the CMNO/PMS system.

Table S1 Textural properties of NMO thermal activation after different temperature.

Thermal activation temperature	S_{BET}	V_{tot}	D_p
°C	m²/g	cm³/g	nm
200	31.67	0.094	10.571
400	33.53	0.056	6.324
600	24.45	0.103	14.622
800	10.98	0.052	12.152

S_{BET}: BET surface area; V_{tot}: total pores volume; D_p: average pore size.
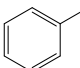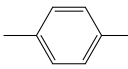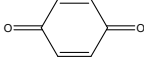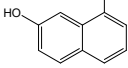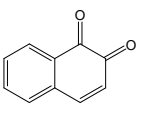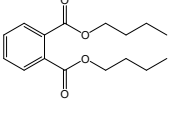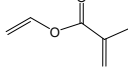
Table S2 The acid amount of NMO and CNMO.

Sample	Acid amount（mmol/g）			The total acid amounts（mmol/g）
	Weak (< 250°C)	Medium (250°C-400°C)	Strong (> 400°C)	
NMO	0.052	0.081	0.481	0.614
CNMO	0.063	0.087	0.538	0.688

Table S3 The total organic carbon (TOC) of actual water.

Actual water	Tap water	Lake water	River water
TOC (mg/L)	1.799	2.560	2.135

Table S4 Possible intermediates of AO7 degradation.

No.	Compound name	Molar mass	Tentative structure	RT (min)
P1	toluene	92		3.150
P2	p-xylene	106		4.680
P3	p-benzoquinone	108		5.535
P4	1,7-dihydroxynaphthalene	160		22.460
P5	1,2-naphthoquinone	158		19.665
P6	dibutyl phthalate	278		26.905
P7	Methacrylic acid, vinyl ester	112		3.640

| P8 | 2,5-Dimethylnonane | 156 | | 6.595 |
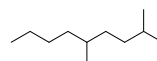
References

1. L. Hou, X. Li, Q. Yang, F. Chen, S. Wang, Y. Ma, Y. Wu, X. Zhu, X. Huang and D. Wang, *Science of The Total Environment*, 2019, **663**, 453-464.

2. J. Deng, S. Feng, X. Ma, C. Tan, H. Wang, S. Zhou, T. Zhang and J. Li, *Separation and Purification Technology*, 2016, **167**, 181-189.

3. J. You, C. Zhang, Z. Wu, Z. Ao, W. Sun, Z. Xiong, S. Su, G. Yao and B. Lai, *Chemical Engineering Journal*, 2021, **415**, 128890.

4. H. Zhou, L. Lai, Y. Wan, Y. He, G. Yao and B. Lai, *Chemical Engineering Journal*, 2020, **384**, 123264.